J. Fluid Mech. (1993), *vol.* 249, *pp.* 59–72

Prandtl–Batchelor flow past a flat plate at normal incidence in a channel – inviscid analysis

By COLIN TURFUS

Department of Mathematics, Sung Hwa University, Cheonan, S. Korea

(Received 23 March 1991 and in revised form 28 September 1992)

A calculation is made of the steady profile adopted by a touching pair of vortex regions with equal and opposite vorticity in a bounded uniform stream. A family of possible solutions is deduced, depending upon the magnitude of a (non-dimensionalized) vorticity parameter. A similar calculation is carried out incorporating a flat plate normal to the stream at the upstream end of the vortex configuration. The requirement of tangential separation at the plate tip selects a unique value of the vorticity. It is found that, as the width of the plate is reduced in relation to that of the channel, the vortex profile asymptotically approaches one member of the above-mentioned family. The asymptotic form of the flow in the vicinity of the plate is deduced for this case and compared with a previous calculation.

1. Introduction

There is a good deal of current interest in incompressible planar flows involving regions of uniform vorticity. As Smith (1986) points out, this is for two reasons. The first is an interest in modelling approximately complex vortex flows, which have hitherto tended to be modelled by singular distributions (points, lines and sheets). The second is the demonstration by Batchelor (1956) that such flows can represent the limiting form of separated flows with closed streamlines as the Reynolds number $Re \rightarrow \infty$, i.e. they are so-called 'Prandtl–Batchelor' flows.† A good recent example in the first category is the work of O'Malley *et al.* (1991) on the flow past a backward-facing step. The present work, however, belongs to the second category.

The review of Smith (1986) illustrates how slow was the progress in tracking down examples of Prandtl–Batchelor flow. A couple of early contenders were Childress's (1966) slender-eddy model of unbounded flow over a backward-facing step and Sadovskii's (1971) calculation of the steady profile adopted by a touching pair of vortex regions with equal and opposite vorticity in unbounded uniform flow. Recently a larger number have emerged. However, most of these inviscid flow configurations either fail, or at least have not yet been shown to pass, the test of demonstrating themselves to be limit solutions of the Navier–Stokes equations.

For example, Childress's (1966) inviscid model was criticized by Chernyshenko (1984) on the grounds that the incorporation of viscous effects led to a predicted unfavourable pressure gradient upstream of the step, which phenomenon is inconsistent with the original assumption of smooth separation from the step. Calculations by Saffman & Tanveer (1984) and Pullin (1984) do not give consideration to the question of whether the derived inviscid flow is a large-Re limit. Chernyshenko

† The term is used by some authors in the above sense, but also in the broader sense of a steady inviscid flow involving regions of constant vorticity. We shall restrict ourselves to the narrower interpretation, it being more in keeping with the spirit of Batchelor's (1956) work.

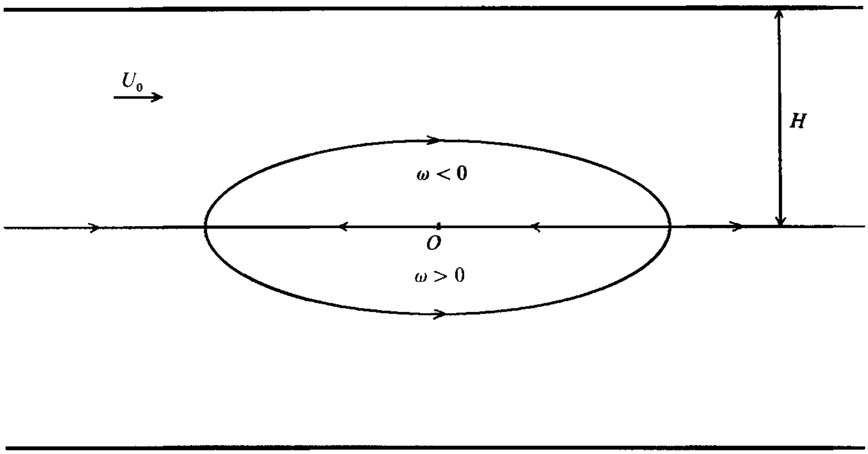

FIGURE 1. Schematic diagram of touching vortices in a channel.

(1982, 1984) considers two-dimensional flow past a rectangular cavity in a plane surface and plane stagnation flow with a normal flat plate attached to the plane at the stagnation point. Values are calculated in each of these cases for the (constant) vorticity in the recirculating region, so as to make the flow consistent with the assumption of its being a large-*Re* limit, but the calculations are necessarily approximate. Furthermore, the author himself expresses reservations about the procedure adopted and admits the likelihood of secondary separations being predicted by more careful analysis.

One exception in this regard is the calculation by Riley (1981) who considered the closed streamline flow in an elliptic region with a prescribed velocity distribution on the boundary. The condition of smooth matching with a constant-vorticity core flow enabled a unique value of the core vorticity to be found.

A more interesting example, however, is that of Sadovskii's (1971) vortex, it having been shown by Smith (1985) and Chernyshenko (1988) how such an inviscid flow configuration could in fact describe the viscous steady wake set up in an unbounded large-*Re* flow past a bluff obstacle. More recent work (Chernyshenko, 1992*b*) indicates how similar arguments apply in the case of bounded flow. It is of interest therefore to calculate how the inclusion of bounding surfaces and a flat plate influence the Sadovskii profile.

In §2 below we consider the effect of the bounding walls on the vortex profile. The calculation is extended in §3 with the inclusion of a flat plate on the centreline of the flow, with the vortices separating from its endpoints. Section 4 considers the limiting case that occurs when the plate becomes vanishingly small, examining in detail the flow in the vicinity of the plate. A closing section discusses whether these inviscid flows with regions of constant vorticity might be the large-*Re* limits of a Navier–Stokes flow.

2. Touching vortices in a channel

Consider the configuration illustrated in figure 1. Two vortex regions with equal vorticity of opposite sign touch along the centreline of a channel of half-width H. The magnitude of their vorticity is ω. We shall specify that there be no drop in Bernoulli constant across the vortex boundary; the velocity is thus everywhere continuous. The vortex regions are assumed to possess reflectional symmetry about their common boundary and about an axis at right angles to it. We take Cartesian coordinates in the direction of these two axes, with the origin of coordinates at the centre of symmetry. We seek, for given values of ω and H, the vortex profiles that permit a *steady* flow solution.

Our method of solution is essentially that used by Saffman & Tanveer (1982), which method originated with Deem & Zabusky (1978). We use the fact that, for a steady solution, the vortex boundary must be a streamline of the flow. In terms of a complex velocity potential

$$W(z) = \phi(x,y)+\mathrm{i}\psi(x,y) \tag{2.1}$$

with $z = x+\mathrm{i}y$, the equation to be solved for the vortex boundary can be expressed as

$$\operatorname{Im} W(z) = 0. \tag{2.2}$$

The required vortex potential is

$$W(z) = U_0 z+\frac{\omega}{4\pi}\sum_{n=-\infty}^{\infty}\left\{\int_C [(z-z_n')\ln(z-z_n')+(z+z_n')\ln(z+z_n')]\,\overline{\mathrm{d}z'}\right.$$
$$\left.+\int_C [(z-\overline{z_n'})\ln(z-\overline{z_n'})+(z+\overline{z_n'})\ln(z+\overline{z_n'})]\,\mathrm{d}z'\right\}, \tag{2.3a}$$

where
$$z_n' = z'+2nH\mathrm{i}, \tag{2.3b}$$

the overbar denotes a complex conjugate and the contour C is that part of the unknown vortex boundary residing in the first quadrant of the complex plane closed by the addition of appropriate sections of the real and imaginary axes (and negotiated in an anticlockwise direction). The influence of the bounding surfaces is represented by an infinite series of identical image vortices with centres at $\pm 2nH\mathrm{i}$, $n = 1,2,\ldots$, which have the effect of rendering $\psi = 0$ when $\operatorname{Im} z = \pm nH$.

We introduce polar coordinates (r,θ) centred on O, in terms of which the boundary can be specified as $\{z\colon z = R(\theta)\,\mathrm{e}^{\mathrm{i}\theta},\ \theta\in[0,\tfrac{1}{2}\pi]\}$ where $R(\theta)$ is to be found. A finite Fourier series approximation for $R(\theta)$ was used:

$$\tilde{R}(\theta) = \sum_{n=0}^{N-1} S_n\cos 2n\theta. \tag{2.4}$$

Equation (2.2) was then satisfied at collocation points $\theta_j = j\pi/2N$, yielding N equations for the N unknowns, S_n.

The integrals in (2.3*a*) were evaluated numerically for $|n| < M$, for some suitable positive integer M. The contributions of more distant vortex pairs were estimated by replacing each with a dipole of equivalent moment at its centre. The contribution to the stream function ψ at position $z = x+\mathrm{i}y$ is of the form

$$\text{constant}\times\operatorname{Im}[2nH\mathrm{i}-z]^{-1}.$$

Combining contributions from $\pm n$ and taking the asymptotic limit as $MH\rightarrow\infty$ (so that $2MH \gg |z|$) we find the total contribution to ψ from distant vortices is

$$\psi_M = \frac{\lambda y}{\pi H^2}\left\{\frac{\pi^2}{6}-\sum_{n=1}^{M}\frac{1}{n^2}\right\}, \tag{2.5}$$

with λ the vortex dipole strength defined in the usual way as

$$\lambda = \iint 2\omega y\,\mathrm{d}x\,\mathrm{d}y,$$

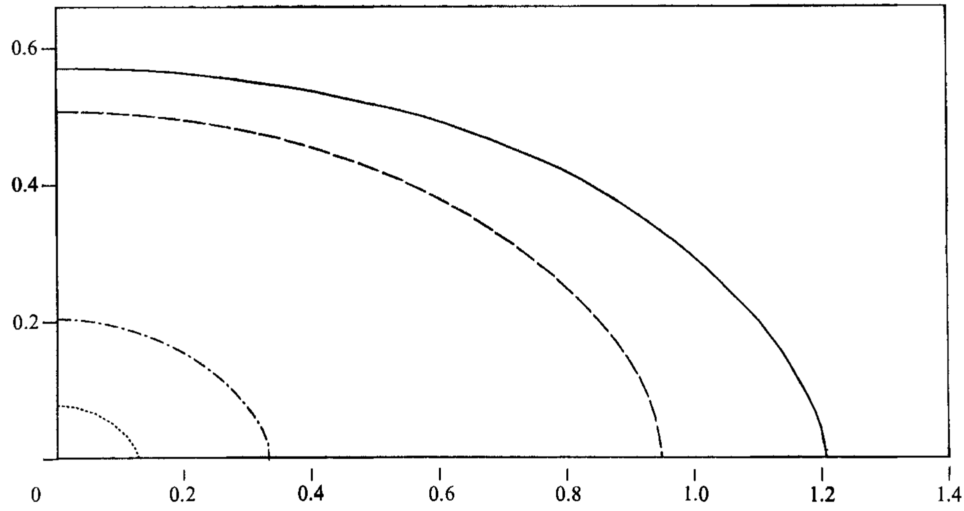

FIGURE 2. Touching vortices in a channel for various values of $\Lambda = |\omega H/U_0|$: $\Lambda = 50$ (.......), $\Lambda = 20$ (—·—), $\Lambda = 10$ (--), $\Lambda = 9.3$ (——).

where the area integral is taken over the upper vortex region. Given ω, U_0, H and a suitable guess for the S_n we can now make an approximate evaluation of the stream function ψ.

We find it convenient at this point to introduce the non-dimensional parameter

$$\Lambda := |\omega H/U_0|. \tag{2.6}$$

The solutions of Sadovskii (1971) correspond to $\Lambda = \infty$. His solution was used as an initial guess in a calculation with $\Lambda = 50$ using $N = 10$ and $M = 2$. A solution was found using a Powell hybrid Newton method from the NAG library, which method employs a combination of Newton and chord iterations. The $\Lambda = 50$ solution was used as an initial guess for a solution with $\Lambda = 20$; this solution was in turn used as an initial guess for a solution with $\Lambda = 10$. Larger values of M up to 30 were found to be required as Λ was decreased in this way.

Solutions for $\Lambda = 10$, 20 and 50 are depicted in figure 2, for fixed H and U_0. As one would expect, the size of the vortices increases and their aspect ratio (width/length) decrease as Λ is decreased. Less obviously, however, the circulation of the vortices increases from $37U_0^2/|\omega|$ for $\Lambda = \infty$ to $72U_0^2/|\omega|$ for $\Lambda = 10$. An increase can be seen to be necessary by means of a simple argument. For, with a decreasing aspect ratio and fixed circulation, the dipole moment, and thus also the self-induced velocity, of a vortex pair will decrease: this would contradict our requirement that U_0 be fixed. Note that this simple argument ignores the increasing influence of the channel walls. However, since their effect is equivalent to that of an array of image vortex pairs, which act against the self-induction, our conclusion is once again that the vortex circulation must increase.

Computational details

Each of the above solutions was obtained with one or two Newton iterations, each followed by up to four chord iterations. After converged solutions were obtained, the value of M was progressively doubled until the vortex length L and width W varied by less than 1% between successive solutions. For $\Lambda = 50$, increasing M above 2 made less than a 0.2% difference. Solutions were also calculated with larger values

Λ	M	N	W/H	L/H	Largest residual
50	2	10	0.078	0.26	$\leqslant 10^{-8}$
20	5	10	0.201	0.664	$\leqslant 10^{-7}$
20	10	10	0.203	0.660	$\leqslant 10^{-7}$
10	15	10	0.472	1.88	$\leqslant 10^{-4}$
10	30	10	0.473	1.90	$\leqslant 10^{-4}$

TABLE 1. Typical computational solutions.

of N but the differences were never greater than 1%. Some typical results are presented in table 1.

For $\Lambda = 50$ and 20 the residuals were essentially roundoff. But for $\Lambda = 10$ they are larger. Solutions were also sought for smaller values of Λ, e.g. $\Lambda = 9.5$, but difficulty was experienced in obtaining converged solutions: residuals could not be reduced below 10^{-2}, which level was not considered acceptable. Increases in N, M and the accuracy of integration did little to improve the situation.

The reason for this difficulty was not at the time apparent, but it was felt that it stemmed from an inadequacy of the Fourier series in representing the vortex boundary. Confirmation of this view was subsequently given by the discovery of solutions, using alternative methods, for lower values of Λ. Some such evidence is presented in §3 below.

But more substantial evidence has since been provided by Chernyshenko (1992*a*) who has solved the identical problem by obtaining a full solution of Poisson's equation on a rectangular grid, using finite differences. In spite of this very different approach, his results for $\Lambda \geqslant 9.3$ appear to corroborate ours to within 1 or 2% (although the values of Λ he considered do not correspond exactly with those considered here). In addition to his numerical results Chernyshenko (1992*a*) proves analytically that $\Lambda = 9$ is a strict lower limit and that, as this value is approached, both the vortex circulation and the vortex aspect ratio L/W are unbounded. Thus, for $9 < \Lambda < 10$, it is seen that no singularities exist in the analytically specified problem and that our difficulties must as a result have stemmed from the discretization, namely the Fourier series approximation.

3. Bounded flow past a flat plate

Since we are interested in the possible applicability of the vortex pair configuration as a model of the flow in the wake of a flat plate, we consider the effects of including a normal flat plate at the upstream end of the vortices. The situation we shall consider is depicted in figure 3. The flow is taken, as in §2, to be symmetric across the channel centreline, the vortex in figure 3 representing the upper half of the flow.

This flow configuration is closely related to that studied by Pullin (1984). He considered unbounded flow past a normal flat plate, where the separation streamline reattaches to an identical normal flat plate positioned a fixed distance downstream of the first. He obtained a family of solutions for different values of the (fixed) drop in Bernoulli constant across the separation streamline, but considered only the case where the plates were positioned $15h$ apart. We of course assume a zero drop in Bernoulli constant; also our interest is mainly in the case where the plate size is very small compared to the vortex dimensions.

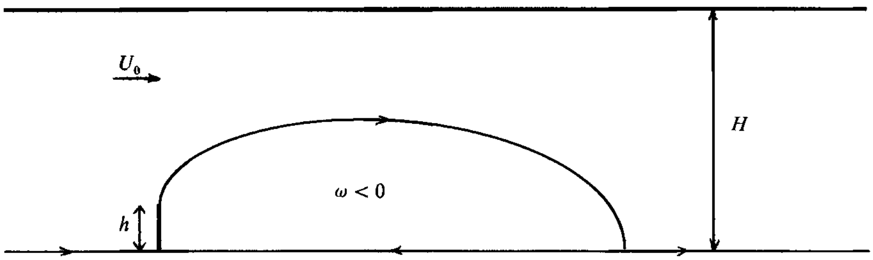

FIGURE 3. Schematic diagram of the wake behind a flat plate in a channel.

Consider then Cartesian coordinates with origin at the centre of symmetry O of the plate and once again define a complex coordinate $z = x + \mathrm{i}y$. Let the half-width of the plate be h so the plate tip is at $z = \mathrm{i}h$. In order to obtain an expression for the stream function, we first carry out a Schwartz–Christoffel conformal mapping of the upper half-channel $\{z\colon \mathrm{Im}\, z \in [0, H]\}$ onto the upper half-ζ-plane. This can be done by setting

$$\frac{\mathrm{d}z}{\mathrm{d}\zeta} = \frac{H}{\pi} \frac{\zeta + 1/(1+\alpha^2)}{(\zeta + 1/(1-\alpha^4))\,[\zeta(1+\zeta)]^{\frac{1}{2}}}, \tag{3.1a}$$

where
$$\alpha = \tan\left\{\frac{\pi(H-h)}{4H}\right\}. \tag{3.1b}$$

Integrating, we obtain

$$z = \frac{H}{\pi} \ln\left\{\frac{((\zeta+1)^{\frac{1}{2}} + \zeta^{\frac{1}{2}})\,((\zeta+1)^{\frac{1}{2}} - \alpha^2\zeta^{\frac{1}{2}})}{((\zeta+1)^{\frac{1}{2}} - \zeta^{\frac{1}{2}})\,((\zeta+1)^{\frac{1}{2}} + \alpha^2\zeta^{\frac{1}{2}})}\right\}. \tag{3.1c}$$

Under this transformation the point $z = 0^+$ is mapped to $\zeta = 0$, $z = 0^-$ to $\zeta = -1$ and $z = \mathrm{i}h$ to $\zeta = -1/(1+\alpha^2)$. The inverse transformation is given by

$$1/\zeta = -1-\alpha^2\left\{\frac{[\cosh\beta(z+z_0)]^{\frac{1}{2}} + [\cosh\beta(z-z_0)]^{\frac{1}{2}}}{[\cosh\beta(z+z_0)]^{\frac{1}{2}} - [\cosh\beta(z-z_0)]^{\frac{1}{2}}}\right\}^2, \quad \mathrm{Re}\,[z] \geqslant 0,$$

$$= -1-\alpha^2\left\{\frac{[\cosh\beta(z+z_0)]^{\frac{1}{2}} - [\cosh\beta(z-z_0)]^{\frac{1}{2}}}{[\cosh\beta(z+z_0)]^{\frac{1}{2}} + [\cosh\beta(z-z_0)]^{\frac{1}{2}}}\right\}^2, \quad \mathrm{Re}\,[z] < 0, \tag{3.2a}$$

where
$$z_0 = H - h, \quad \beta = \pi/2H. \tag{3.2b, c}$$

We calculate the stream function in the first instance in the ζ-plane, since this allows the effects of the bounding walls and of the plate easily to be included. The complex potential associated with a point vortex of strength Γ at position ζ' is given by

$$W(\zeta, \zeta') = \frac{\Gamma}{2\pi\mathrm{i}} \ln \frac{\zeta - \zeta'}{\zeta - \bar{\zeta}'}.$$

The stream function can be calculated by integrating such contributions over the region of non-zero vorticity. Unfortunately, the double integral thus obtained cannot be transformed into a contour integral like (2.3a), since the vorticity, expressed as a function of ζ rather than of z, is no longer constant. Since we must deal with an area integral, we choose to express the region of integration in z-coordinates. This has the advantage that the area of integration is more compact; in addition, the Jacobian for the transformation is the reciprocal of the vorticity weighting function in ζ-space, so our integral once again has constant vorticity. We find

$$W(z) = U_0 z - \frac{\omega}{2\pi \mathrm{i}} \iint \ln \left\{ \frac{\zeta(z) - \zeta(z')}{\zeta(z) - \bar{\zeta}(z')} \right\} \mathrm{d}S(z'), \tag{3.3}$$

where $\zeta(z)$ is as defined in (3.2) and the integration is over the region of non-zero vorticity in the upper half-z-plane. The equation to be solved is once again (2.2), but with two extra conditions at the plate tip. First, we apply a Kutta condition, i.e. we require that the vortex boundary attach to the plate tip at $z = \mathrm{i}h$. Secondly, we demand that the velocity be finite in the vicinity of the plate tip; this will be so only if the vortex boundary attaches parallel to the plate, i.e. if

$$\mathrm{Re}\left[\frac{\mathrm{d}W}{\mathrm{d}z}(z = \mathrm{i}h)\right] = 0 \tag{3.4}$$

(see Smith 1982). The problem to be solved is now completely specified.

To obtain a solution, we again approximate the vortex boundary by a finite Fourier series. Take polar coordinates with origin at $z = (C, 0)$, where $2C$ is an estimate of the vortex length. Then on the boundary $z = R(\theta)\,\mathrm{e}^{\mathrm{i}\theta}$, with $R(\theta)$ to be specified. The plate tip corresponds to $\theta = \theta_m = \pi - \tan^{-1}(h/C)$. Then

$$R(\theta) = -C \sec\theta, \quad \theta_m \leqslant \theta \leqslant \pi. \tag{3.5a}$$

We approximate $R(\theta)$ by

$$\tilde{R}(\theta) = \sum_{n=0}^{N-1} S_n \cos(n\eta(\theta)), \quad 0 \leqslant \theta < \theta_m, \tag{3.5b}$$

where the stretching function $\eta(\theta)$ is defined according to

$$\tan\theta = \gamma \tan\eta(\theta) \tag{3.5c}$$

and γ is a constant which should be chosen roughly equal to double the aspect ratio of the vortex to ensure that the collocation points are fairly evenly spaced along the vortex boundary. (In practice a value of $\frac{1}{3}$ was used, weighting the density of collocation points slightly towards the ends of the vortex, where the curvature is greater.)

Now define collocation points θ_j, $j = 1, N-1$ for θ in the range $(0, \theta_m)$ by setting

$$\tan\theta_j = \gamma \tan(\eta(\theta_m) j/N), \quad j = 1, 2, \ldots, N-1. \tag{3.6}$$

Satisfying (2.2) at the collocation points gives $N-1$ equations. Matching (3.5*a*) and (3.5*b*) at $\theta = \theta_m$ gives another. Equation (3.4) is equivalent to an $(N+1)$th equation:

$$\frac{\mathrm{d}R}{\mathrm{d}\theta}(\theta = \theta_m) = C \sec\theta_m \tan\theta_m = -\frac{h}{C}(C^2 + h^2)^{\frac{1}{2}}. \tag{3.7}$$

These equations we must now solve for the $N+1$ unknowns, namely S_n, $n = 0, 1, \ldots, N-1$ and $\Lambda = |\omega H/U_0|$. We seek a solution, in the first instance for $h/H = 0.1$, taking as initial guess our solution from §2 with $\Lambda = 10$. A Newton method was once again employed. The integral in (3.3) was evaluated numerically using an adaptive integrating routine capable of dealing with the logarithmic singularities in the integrand which occur at the collocation points. With $N = 18$ an evaluation of (3.3) took about 1 minute of CPU time on a SUN SPARC station. A calculation based on 2 evaluations of the Jacobian and 8 chord steps typically took 18 hours.

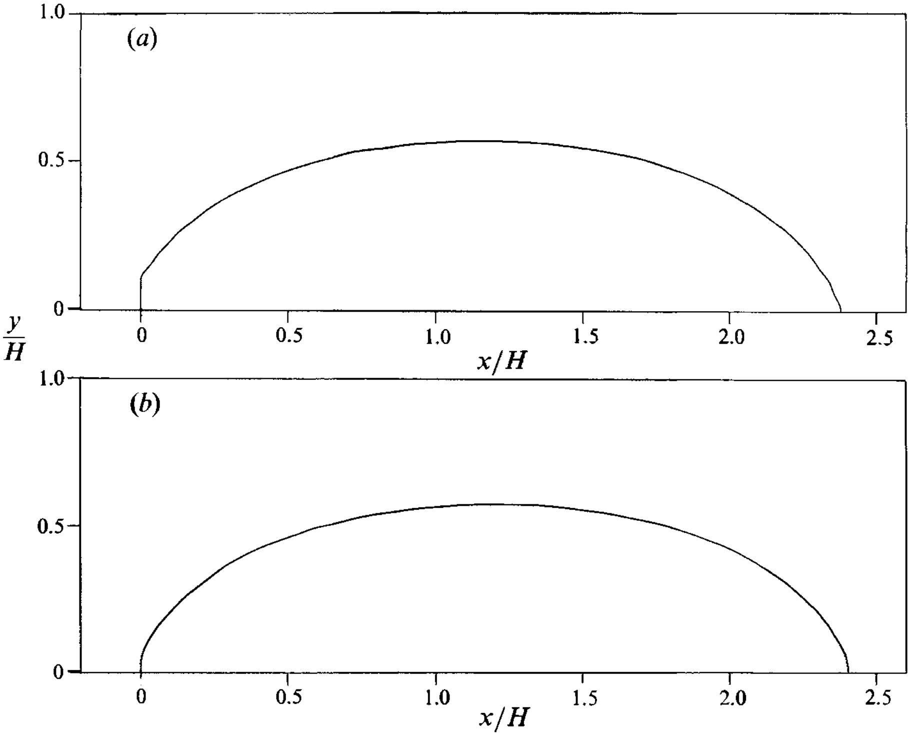

FIGURE 4. Constant-vorticity wake behind a flat plate in a channel: (a) $h/H = 0.1$, (b) $h/H = 0.01$.

Some difficulty was experienced in obtaining converged solutions, mainly on account of the extremely sensitive derivative condition (3.7) applied at the fence tip. Even when calculations converged, it was found that our discretized version of (2.2) did not have proper zeros: rather there remained residuals with a magnitude of up to $0.005U_0 H$. It was concluded that this was on account of the inability of the Fourier series adequately to represent the infinite curvature of the separation streamline at the plate tip (see Smith 1982).

Greater accuracy was sought by using larger values of N; the required CPU time increased as N^2. A calculation was carried out for the case $h/H = 0.01$ with $N = 80$. Unfortunately, even with this large increase in the value of N, the magnitude of the residuals did not diminish. However, since it was observed that neither the vortex shape nor the predicted value of Λ were much affected by the increase in N, it was concluded that these properties could be taken as having been reliably predicted, the only real uncertainty being in the precise nature of the flow in the near vicinity of the plate tip. This regime is considered in greater detail in §4 below.

The value of Λ was, somewhat surprisingly, found to be 9.3 for all values of h/H up to 0.1. The vortex profiles obtained for $h/H = 0.1$ with $N = 45$ and for $h/H = 0.01$ with $N = 80$ are illustrated in figure 4. As can be seen, the latter profile is almost perfectly symmetric and was taken to be representative of the limit as $h/H \to 0$. The profile for $h/H = 0.1$ is little different, except of course near the plate.

Comparing the limit solution for $\Lambda = 9.3$ with the $\Lambda = 10$ solution from §2, we find a decrease in aspect ratio from 0.275 to 0.24; the associated increase in Γ is from $72U_0^2/|\omega|$ to $99U_0^2/|\omega|$.

4. Asymptotic analysis near the plate

We now consider in more detail the flow structure near the plate in the limit as $h/H \to 0$. This we shall do in three stages, by first considering the case $h = 0, H = \infty$, then examining the effect of introducing a non-zero value of h and finally letting H be finite. It will be seen that, although the second of these cases ($h \neq 0, H = \infty$) does not yield a consistent asymptotic structure, consistency can none the less be restored in the third case when a finite value of H is employed.

4.1. $h = 0, H = \infty$

We start our asymptotic analysis by considering the flow that results when the vortex size (as measured by the parameter $|U_0/\omega|$) is constrained to be small compared to the channel width, but large compared to the plate size. In other words we take the asymptotic limit as $\omega h/U_0 \to 0$ and $\Lambda = |\omega H/U_0| \to \infty$. We argue that the flow structure (on the scale $|U_0/\omega|$) must become independent of both h and H and must therefore tend towards the Sadovskii (1971) profile discussed above. To examine how such a vortex profile might be joined to a plate on the lengthscale $O(h)$, we must consider the asymptotic structure of that flow in the near vicinity of the front stagnation point.

The necessary calculation has in fact been carried out by Saffman & Tanveer (1982), whose analysis we shall now seek to extend. They take the front stagnation point of the vortex to be the origin of polar coordinates (r, θ) with flow from right to left. We shall follow their convention for the purposes of the present analysis, since it yields a certain elegance of notation (see figure 5). Their result for the stream function can be conveniently expressed as

$$\psi(z) = \operatorname{Im} \frac{\omega}{2\pi} \left\{ z^2 \ln \frac{z}{y_0} - \mathrm{i}\pi r^2 \cos^2\theta \,\mathrm{H}\left(\theta - \frac{\pi}{2}\left(1 - \frac{1}{1+2\ln(r/y_0)}\right)\right) + O(z^2/\ln(z/y_0)) \right\} \quad \text{as} \quad z \to 0, \tag{4.1a}$$

where H(.) is the Heaviside step function.

The constant y_0 was not determined in the analysis of Saffman & Tanveer (1982), but further computation by this author, employing 400 points (instead of Saffman & Tanveer's 20) in the specification of the vortex boundary, has shown that

$$y_0 = 8.8|U_0/\omega| \tag{4.1b}$$

to an accuracy of about 5%.

We start by noting that the result (4.1 *a*) is deducible from the assumption of a formal asymptotic expansion of the form:†

$$\psi(z) = \operatorname{Im} \frac{\omega}{2\pi} \left\{ z^2 \ln \frac{z}{y_0} + \sum_{n=1}^{\infty} \frac{A_n z^2}{(\ln(z/y_0))^n} \right\} \quad (0 \leqslant \theta \leqslant \tfrac{1}{2}\pi + \delta(r)) \tag{4.2a}$$

$$= \operatorname{Im} \frac{\omega}{2\pi} \left\{ z^2 \ln \frac{z}{y_0} - \mathrm{i}\pi r^2 \cos^2\theta + \sum_{n=1}^{\infty} \frac{B_n z^2}{(\ln(-z/y_0))^n} \right\} \quad (\tfrac{1}{2}\pi + \delta(r) < \theta \leqslant \pi), \tag{4.2b}$$

with

$$\delta(r) = \sum_{n=1}^{\infty} \frac{\delta_n}{|\ln(r/y_0)|^n}. \tag{4.2c}$$

† There is a slight discrepancy between this expansion and that deduced by Saffman & Tanveer (1982) in the appearance of terms involving powers of $1/\ln(-z/y_0)$ in (4.2 *b*). This form is necessary to satisfy the boundary condition on $\theta = \pi$, which condition is not in fact satisfied by the expansion of Saffman & Tanveer (1982).

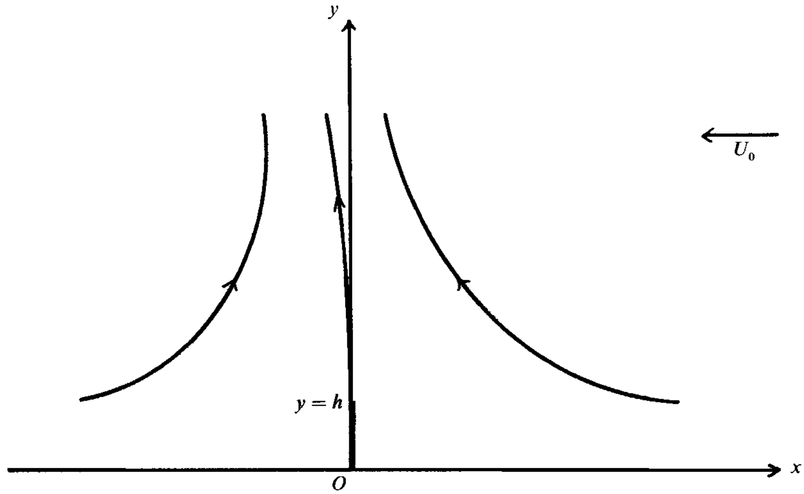

FIGURE 5. Definition sketch for asymptotic analysis near plate.

The equation satisfied by (4.2) is

$$\begin{aligned}\nabla^2\psi &= 0 \quad (0 \leqslant \theta \leqslant \tfrac{1}{2}\pi+\delta(r))\\ &= -\omega \quad (\tfrac{1}{2}\pi+\delta(r) < \theta \leqslant \pi),\end{aligned} \tag{4.3}$$

with boundary conditions that $\psi = 0$ on $\theta = 0$, $\frac{1}{2}\pi+\delta(r)$ and π, and further that $\partial\psi/\partial\theta$ is continuous on $\theta = \frac{1}{2}\pi+\delta(r)$.

The form of (4.2) ensures that the boundary conditions at $\theta = 0$ and π are automatically satisfied. The boundary conditions at $\theta = \frac{1}{2}\pi+\delta(r)$ specify three further relations between the δ_n, A_n and B_n. Matching of terms proportional to $|\ln(r/y_0)|^{-n}$ for successive values of n allows the constants to be successively determined, in principle for any value of n. The procedure appears to be self-consistent and yields

$$\begin{aligned}
&\delta_1 = \tfrac{1}{4}\pi, && A_1 = -\tfrac{1}{12}\pi^2,\\
&\delta_2 = \tfrac{1}{8}\pi, && B_1 = \tfrac{1}{6}\pi^2,\\
&\delta_3 = \tfrac{1}{16}\pi+\tfrac{1}{48}\pi^3, && A_2 = 0,\\
&\delta_4 = \tfrac{1}{32}\pi, && B_2 = -\tfrac{1}{8}\pi^2,
\end{aligned}$$

consistent also with the results of Saffman & Tanveer (1982).

4.2. $h \neq 0$, $H = \infty$

We next examine how this asymptotic structure is influenced by the inclusion of a small flat plate of half-width h ($\ll y_0$) inclined normally to the flow at the point of separation. We insist that the flow separate tangentially from the plate tip and that there be no Bernoulli drop across the separation streamline, as assumed in §2 above. Equation (4.3) again applies with the same boundary conditions. Of course now $\delta(r) = 0$ for $r \leqslant h$.

We seek a local solution in the vicinity of the plate under the assumption that the stream function tend asymptotically to the Saffman & Tanveer (1982) solution, which we shall henceforth refer to as the '$h = 0$' solution. Thus we suppose

$$\psi(z) = \mathrm{Im}\frac{\omega}{2\pi}\left\{z^2\ln\frac{z}{y_0} - \mathrm{i}\pi r^2\cos^2\theta\,\mathrm{H}(\theta-\tfrac{1}{2}\pi-\delta(r))\right\}+\psi_{\mathrm{H}}, \tag{4.4a}$$

where ψ_H is a harmonic function satisfying:

$$\psi_H = o(|z|^2) \quad \text{as} \quad |z|/h \to \infty, \tag{4.4b}$$

and seek solutions for ψ_H and $\delta(r)$, such that (4.4*a*) asymptotically satisfies (4.3) and the associated boundary conditions. The former is most readily found by a conformal mapping into the ζ^*-plane, where

$$\zeta^* = \rho\, e^{i\phi} = (z^2+h^2)^{\frac{1}{2}}. \tag{4.5}$$

The problem for ψ_H can then be expressed as

$$\nabla^2\psi_H = 0, \tag{4.6a}$$

$$\psi_H = 0, \quad \phi = 0, \pi, \quad \rho > h, \tag{4.6b}$$

$$\psi_H = \tfrac{1}{4}\omega(h^2-\rho^2), \quad \phi = 0,\pi, \quad \rho \leqslant h, \tag{4.6c}$$

$$\psi_H = o(\rho^2) \quad \text{as} \quad \rho \to \infty. \tag{4.6d}$$

The solution is straightforward. We find

$$\psi_H(z) = \operatorname{Im}\frac{\omega}{4\pi}\left\{(\zeta^{*2}-h^2)\ln\frac{\zeta^*+h}{\zeta^*-h}+B\zeta^*\right\}, \tag{4.7}$$

where B is a constant. (A second complementary function proportional to ζ^{*2} has been ignored since it is not $o(|z|^2)$ and has effectively already been included in (4.4*a*).) From (4.4*a*) and (4.7) we conclude that

$$\psi(z) \sim \operatorname{Im}\frac{\omega}{2\pi}\left\{z^2\ln\frac{(z^2+h^2)^{\frac{1}{2}}+h}{y_0}+B(z^2+h^2)^{\frac{1}{2}}-i\pi r^2\cos^2\theta\,\mathrm{H}(\theta-\tfrac{1}{2}\pi-\delta(r))\right\}. \tag{4.8}$$

It remains to specify the value of the constant B and the required form of the function $\delta(r)$. Consideration of the behaviour of $\partial\psi/\partial\theta$ near $z = ih$ shows that it becomes singular there, unless

$$B = h, \tag{4.9}$$

which value we therefore take as appropriate in order to satisfy the condition of tangential separation at the plate tip.

The form of $\delta(r)$ is most readily obtained by consideration of the function $\delta^*(\rho)$ defined by

$$\delta^*(\rho) = \arg(\zeta^*)-\tfrac{1}{2}\pi \tag{4.10}$$

for any point ζ^* on the separation streamline in the image plane. This is related to $\delta(r)$ by

$$\tan 2\delta^*(\rho) = \frac{\sin 2\delta(r)}{h^2/r^2-\cos 2\delta(r)}. \tag{4.11}$$

Thus we can set $\zeta^* = \rho\, e^{i(\pi/2+\delta^*)}$, substitute into (4.8) and use the condition $\psi \sim 0$ to obtain

$$-\tfrac{1}{2}\rho^2\sin 2\delta^*\ln\frac{\rho^2+h^2-2h\rho\sin\delta^*}{y_0^2}$$

$$-(\rho^2\cos 2\delta^*+h^2)\tan^{-1}\frac{\rho\cos\delta^*}{h-\rho\cos\delta^*}+h\rho\cos\delta^* \sim 0. \tag{4.12}$$

We have neglected the particular integral proportional to $\pi r^2\cos\theta$ since it is

$O(\rho^4\delta^{*2}/(\rho^2+h^2))$ as $\delta^* \to 0$ and, as we shall see, gives a negligible contribution to ψ to the order of accuracy of our calculation. We pose the following expansion for $\delta^*(\rho)$:

$$\delta^*(\rho) = \sum_{n=1}^{\infty} \frac{f_n(\rho/h)}{|\ln[(\rho^2+h^2)^{\frac{1}{2}}/y_0]|^n} \tag{4.13a}$$

and substitute into (4.12), gathering together powers of $|\ln[(\rho^2+h^2)^{\frac{1}{2}}/y_0]|$ to obtain, at $O(1)$,

$$f_1(x) = \frac{1}{2}\left\{\frac{1+x^2}{x^2}\tan^{-1}x - \frac{1}{x}\right\}, \tag{4.13b}$$

and at $O(|\ln[(\rho^2+h^2)^{\frac{1}{2}}/y_0]|^{-1})$:

$$f_2(x) = \tfrac{1}{2}f_1(x). \tag{4.13c}$$

Higher terms were not sought, since they would require matching with the neglected particular integral, which is discontinuous at $\phi = \frac{1}{2}\pi + \delta^*$ and so would require in turn an additional (discontinuous) complementary function to render the procedure consistent.† We observe that

$$f_1(\rho/h) \sim \rho/3h \sim 0 \quad \text{as} \quad \rho/h \to 0, \tag{4.14a}$$

and that

$$f_1(\rho/h) \sim \tfrac{1}{4}\pi \quad \text{as} \quad \rho/h \to \infty, \tag{4.14b}$$

as is required for asymptotic matching with the outer solution. The condition on $\partial\psi/\partial\theta$ is automatically satisfied to the assumed level of approximation, since ψ is continuous. The expansion (4.8) with (4.9), (4.11) and (4.13) is thus seen to be consistent.

We next go on to compare (4.8) in the limit as $|z|/h \to \infty$ with the $h = 0$ solution (4.2). We have, from (4.8),

$$\psi(z) \sim \operatorname{Im}\frac{\omega}{2\pi}\left\{z^2 \ln\frac{z}{y_0} + 2hz - \mathrm{i}\pi r^2 \cos^2\theta\, \mathrm{H}(\theta - \tfrac{1}{2}\pi - \delta(r))\right\}$$
$$\text{as} \quad |z|/h \to \infty, \quad |z|/y_0 \to 0, \tag{4.15}$$

where the function $\delta(r)$ is now asymptotically equivalent to the corresponding function appearing in the $h = 0$ solution. Aside from the obvious discrepancy with the A_n and B_n, which we were able to ignore in our inner expansion, there is a further discrepancy in the appearance of a term $2hz$ in (4.15). We recall that this term's inclusion is necessary to ensure a velocity field which is non-singular in the vicinity of the plate tip. However, its appearance would at the same time appear to preclude asymptotic matching with the outer flow for *any* value of h. This does not immediately preclude the possibility of the plate having a non-perturbation effect on the outer flow. But since, for any given h, there is only one free parameter in the flow, namely $\omega h/U_0$, and since, in general, only one value of the parameter will yield a singularity-free velocity field, there would appear to be insufficient degrees of freedom to support such a flow, except in the limit as $\omega h/U_0 \to 0$, which is, of course, the $h = 0$ case. We deduce that it is not possible to join a Sadovskii-type region of constant vorticity to a plate in unbounded flow, while maintaining the condition of tangential separation.

† An attempt was in fact made to derive a uniformly valid asymptotic expansion which matched with the higher-order terms involving A_n and B_n in (4.2). However, no suitable extension of (4.8) could be found which did not lead to inconsistent predictions for $f_3(x)$. The question of the (possible) form of higher-order terms in (4.8) thus remains open.

4.3. $h \neq 0, H \neq \infty$

This need not be the case, however, for our bounded flow problem. For, as we found in §3 above, it appears always to be possible, when the plate is positioned in a channel of arbitrary half-width H, to satisfy the condition of tangential separation by suitably adjusting the value of the vorticity ω. The *local* solution is then identical in almost every respect to the one just discussed, the one exception being in the value of y_0, which should be recalculated from an inviscid flow calculation on the lengthscale of the large vortex in the new geometry (see §3 above).

Unfortunately, this was not possible in practice, since the vortex boundary in the calculation of §3 was not well enough resolved. However, comparing with the calculation for $h = 0$, $H \equiv \infty$ in §4.1 above, we must expect that once again

$$y_0 = O(U_0/\omega).$$

If we further assume the same constant of proportionality as in (4.1*b*) and use the computed value $\Lambda = 9.3$ from §3, we obtain the estimate $y_0 = 0.91H$. Thus, in the absence of further information, we follow the simple expedient of identifying y_0 and H, i.e. we estimate:

$$y_0 = H \tag{4.16}$$

with consequent errors of $O(1)$ in the value of $\ln(h/y_0)$. We deduce the following expression for the velocity on the front *and* on the back of the plate:

$$v(0,y) = -\frac{\omega y}{\pi}\left\{\ln\frac{(h^2-y^2)^{\frac{1}{2}}+h}{H}+O(1)\right\} \quad (0 \leqslant y \leqslant h) \tag{4.17}$$

in obvious notation (where in principle the $O(1)$ constant could be calculated).

We can also now offer an interpretation of the $2hz$ term which appears in the stream function in the far field (see (4.15)). This represents a steepening of the trajectory of the separation streamline. Obviously this streamline must eventually flatten out and lie *inside* the original ($h = 0$) streamline in order that the vortex's self-induced velocity remain fixed and equal to U_0. In other words, the vortex should become slightly narrower under the influence of the plate. However, as can be seen from figure 4, this effect would appear to be very slight even for values of h/H as large as 0.1.

In conclusion, we have shown that the corner flow of a vortex separating from a plate of half-width h on the centreline of a channel of half-width H in the limit as $h/H \to 0$ can be described in terms of an inner and an outer expansion.

The outer expansion, applicable when $h \ll |z| \ll y_0$, is given by (4.2), where the value of y_0 has not been calculated (but is $O(H)$), and the first few A_n, B_n and δ_n are given. From (4.15), a term proportional to $2hz$, representing the effect of the finite plate size, should strictly also be included inside the braces in the expressions (4.2*a*, *b*) for ψ.

The inner expansion, applicable when $|z| \ll y_0$, is given by (4.8ff). In fact this 'inner' expansion is strictly a uniform expansion, being applicable throughout the domain of the outer expansion.

5. Concluding remarks

We have shown how the steady profile adopted by a touching pair of vortex regions with equal and opposite vorticity is affected by the presence of bounding walls. Profiles were calculated for various values of the parameter $\Lambda = |\omega H/U_0|$. It was found that, as Λ decreased, the aspect ratio of the vortices decreased and the circulation increased.

The calculation was extended to include a normal flat plate at the upstream end of the vortices. It was shown how the condition of tangential separation from the plate tip selected a unique value of Λ. The value of Λ in the limit as $h/H \rightarrow 0$ was found to be 9.3; negligible change in Λ was found for values of h/H up to 0.1.

The flow near the plate was examined asymptotically for the limiting case $h/H \rightarrow 0$. An expression was derived (equation (4.17)) for the fluid velocity on the surface of the plate. The influence of the plate on the separation streamline was examined (equation (4.15)) and was found to extend into the far field.

We return finally to the question raised in §1 above of whether the inviscid flows discussed are Prandtl–Batchelor limit flows. This requires examination of the effect of finite Re in the boundary layer surrounding the large vortices. Such considerations are beyond the scope of the present paper but have been examined elsewhere. Thus it has been found that the flows described in §2 above all represent inviscid limits, in the sense that they result if we let $Re \rightarrow \infty$, but with Reh/H fixed (Chernyshenko 1992*b*). However, current work by the author shows that the flows described in §3 with a flat plate included appear not to be of the Prandtl–Batchelor type.

The author is grateful to Professor I. P. Castro and Dr P. J. Aston for numerous discussions and invaluable suggestions. The work was jointly sponsored by the SERC, by the Atomic Energy Authority, Harwell, by the Departments of Mechanical Engineering and of Mathematical and Computing Sciences at the University of Surrey, and by the Faculty of Science and Engineering, Sung Hwa University, Cheonan, S. Korea.

REFERENCES

Batchelor, G. K. 1956 *J. Fluid Mech.* **1**, 177.

Chernyshenko, S. I. 1982 *Izv. Akad. Nauk SSR, Mekh, Zhidk, Gaza* **1**, 10–15 (available in English translation).

Chernyshenko, S. I. 1984 *Izv. Akad. Nauk SSR, Mekh, Zhidk, Gaza* **2**, 40–45 (available in English as 'The calculation of separated flows of low-viscosity liquids using the Batchelor model'. *R. Aircraft Establ. Library Transl.* 2133).

Chernyshenko, S. I. 1988 *Appl. Math. Mech.* **52**, 746.

Chernyshenko, S. I. 1992*a* Stratified Sadovskii flow in a channel. *J. Fluid Mech.* (submitted).

Chernyshenko, S. I. 1992*b* High Reynolds-number asymptotics of the stationary flow through a row of bluff bodies. *J. Fluid Mech.* (submitted).

Childress, S. 1966 *Phys. Fluids* **9**, 860.

Deem, G. S. & Zabusky, N. 1978 *Phys. Rev. Lett.* **40**, 859.

O'Malley, K., Fitt, A. D., Jones, T. V., Ockendon, J. R. & Wilmott, P. 1991 *J. Fluid Mech.* **222**, 139–155.

Pullin, D. I. 1984 *Q. J. Mech. Appl. Maths.* **37**, 619.

Riley, N. 1981 *J. Engng. Maths.* **15**, 15–27.

Sadovskii, V. S. 1971 *Appl. Math. Mech.* **35**, 729.

Saffman, P. G. & Tanveer, S. 1982 *Phys. Fluids* **25**, 1929.

Saffman, P. G. & Tanveer, S. 1984 *J. Fluid Mech.* **143**, 351–365.

Smith, F. T. 1985 *J. Fluid Mech.* **155**, 175.

Smith, J. H. B. 1982 In *Vortex Motion*, (ed. H. G. Hornung & E.-A. Müller), pp. 157–172. Vieweg.

Smith, J. H. B. 1986 *Ann. Rev. Fluid Mech.* **18**, 221.